Pertanika J. Sci. & Technol. 28 (S2): 299 - 316 (2020)

SCIENCE & TECHNOLOGY

Journal homepage: http://www.pertanika.upm.edu.my/

Parameters Optimization in Compression Molding of Ultra-high Molecular Weight Polyethylene/Cellulose Nanofiber Bio-nanocomposites by using Response Surface Methodology

Nur Sharmila Sharip[1], Hidayah Ariffin[1,2]*, Yoshito Andou[3], Ezyana Kamal Bahrin[2], Mohammad Jawaid[4], Paridah Md Tahir[5] and Nor Azowa Ibrahim[6]

[1]Laboratory of Biopolymer and Derivatives, Institute of Tropical Forestry and Forest Products (INTROP), Universiti Putra Malaysia, 43400 UPM Serdang, Selangor, Malaysia
[2]Department of Bioprocess Technology, Faculty of Biotechnology and Biomolecular Sciences, Universiti Putra Malaysia, 43400 UPM Serdang, Selangor, Malaysia
[3]Department of Biological Functions and Engineering, Graduate School of Life Science and Systems Engineering, Kyushu Institute of Technology, 2-4 Hibikino, Wakamatsu-ku, Kitakyushu, Fukuoka 808-0196, Japan
[4]Laboratory of Biocomposite Technology, Institute of Tropical Forestry and Forest Products (INTROP), Universiti Putra Malaysia, 43400 UPM Serdang, Selangor, Malaysia
[5]Laboratory of Sustainable Bioresource Management, Institute of Tropical Forestry and Forest Products (INTROP), Universiti Putra Malaysia, 43400 UPM Serdang, Selangor, Malaysia
[6]Department of Chemistry, Faculty of Sciences, Universiti Putra Malaysia, 43400 UPM Serdang, Selangor, Malaysia

ABSTRACT

Conventional UHMWPE molding involves long pressure holding duration, nevertheless in the presence of filler such as cellulose nanofiber (CNF), this may contribute to filler degradation. This study optimized the compression molding parameters of UHMWPE/CNF bio-nanocomposite by using response surface methodology (RSM) in consideration of temperature, pressure and duration as variables. An optimal processing condition of 180°C, 15 MPa, and 20 minutes contributed to more than 80% desirability with tensile strength, yield strength, elongation at break, and Young's modulus values of 22.83 MPa, 23.14 MPa, 487.31%, and 0.391 GPa, accordingly. Mechanical properties of UHMWPE/CNF bio-nanocomposites molded at optimized processing conditions were comparably similar to those prepared at conventional processing condition, and with the advantage of having shorter

ARTICLE INFO

Article history:
Received: 10 February 2020
Accepted: 13 November 2020
Published: 31 December 2020

DOI: https://doi.org/10.47836/pjst.28.S2.23

E-mail addresses:
nursharmilasharip@gmail.com (Nur Sharmila Sharip)
hidayah@upm.edu.my (Hidayah Ariffin)
yando@life.kyutech.ac.jp (Yoshito Andou)
ezyana@upm.edu.my (Ezyana Kamal Bahrin)
jawaid@upm.edu.my (Mohammad Jawaid)
parida.introp@gmail.com (Paridah Md Tahir)
norazowa@upm.edu.my (Nor Azowa Ibrahim)
* Corresponding author

ISSN: 0128-7680
e-ISSN: 2231-8526

processing time. The results presented herewith provides insight towards a more practical approach for UHMWPE/CNF bio-nanocomposites consolidation process.

Keywords: Bio-nanocomposite, cellulose nanofiber, compression molding, optimization, response surface methodology, ultra-high molecular weight polyethylene

INTRODUCTION

Possessing various excellent properties, ultra-high molecular weight polyethylene (UHMWPE) has been used for various application of aerospace, industrial machineries, microelectronic and medical fields (Li et al., 2017; Raghuvanshi et al., 2012), where it is consolidated into many different products including pipes, panels, gears, body armors, unlubricated bearings and artificial joint component (Khalil et al., 2016; Wang et al., 2018). This engineered thermoplastic is made of a repeating unit of ethylene with molecular weight ranged between 3.5 to 7.5 million g/mol (Kurtz, 2016a). The extremely long and linear structure of UHMWPE enables it to greatly withstand impact and abrasion beside having a very low friction (Chukov et al., 2014; Paxton et al., 2019). Not only that, a lot of studies have been conducted on manufacturing UHMWPE nanocomposites for enhanced properties befitting its applications, including UHMWPE/nanocellulose as artificial joint component (Wang et al., 2016).

While various approaches can be adopted in manufacturing and processing the UHMWPE and/or its composites, the consolidation process is restricted to compression molding and ram extrusion. This is stemmed from very low melt flow index of UHMWPE (0.006 g/min) causing other methods such as injection molding and screw extrusion to be not practical (Kurtz, 2016b; Panin et al., 2017). In comparison to other consolidation method, compression molding is considered more practical and well adapted, especially for molding UHMWPE polymer. Differing from other polymers including conventional polyethylene such as low-density polyethylene or high-density polyethylene, UHMWPE comprises extremely long chains leading to very high melt viscosity and slow diffusion during consolidation (Fu et al., 2010; Gao & Fu, 2019). Hence, UHMWPE molding requires a long pressure holding duration, in order to give adequate time for UHMWPE resin to diffuse with each other and create satisfactory entanglements thus good mechanical properties (Kurtz et al., 1999; Parasnis & Ramani, 1998). Besides, Kurtz (2016b) further described that long duration of hot pressing was necessary due to the relatively low thermal conductivity of UHMWPE.

Nevertheless, long duration molding could be a disadvantage, which may expose polymer to degradation (Campo, 2008), especially in consolidation of UHMWPE containing cellulose nanofiber (CNF) fillers. Appropriate compression molding parameters are essentially needed for polymer diffusion and filler impregnation into the matrix (Xie et al., 2019) while avoiding polymer degradation. Meanwhile, in order to improve its

productivity, the shorter duration is imperative for more effective processing. The effect, conjugated with interaction between the varied parameters, wields an impact towards the quality and mechanical properties of UHMWPE/CNF bio-nanocomposites. Therefore, this study optimized the temperature pressure and duration of compression molding for desirably good mechanical properties. The individual and interaction effects of each variables on UHMWPE/CNF bio-nanocomposites mechanical properties were also investigated.

MATERIALS AND METHODS

Materials

Fine UHMWPE powder (Sigma-Aldrich, USA) with average molecular weight of 3 x 10^6 – 6 x 10^6 g/mol was used in this experiment. Maleic anhydride-*grafted*-polyethylene (MAPE) in pellet form was from the same manufacturer by which it contains approximately 0.5 wt.% maleic anhydride. The melting point and density of UHMWPE and MAPE are 138°C, 0.94 g/mL and 107°C, 0.92 g/mL, respectively. The CNF in slurry form was purchased from ZoepNano Sdn. Bhd., Malaysia with concentration of 2 wt.% solid content and average diameter of 50 nm.

Bio-nanocomposite Fabrication and Molding

UHMWPE/ 3 wt.% CNF/ 3 wt.% MAPE bio-nanocomposite was prepared by using triple screw kneading extruder (Imoto Machinery Co., Ltd., Japan) at temperature 150°C, 60 rpm and 45 minutes melt blending condition. Fabricated bio-nanocomposite was then subjected to compression molding at varied parameters of temperature, pressure and duration.

Mechanical Properties of Bio-nanocomposites

Tensile specimen was prepared from compressed bio-nanocomposite film according to ASTM D638. The test was conducted on compact tensile and compression tester IMC-18E0 (Imoto Machinery Co., Ltd., Japan) at 50 mm/min crosshead speed) (ASTM, 2003). The mechanical properties of bio-nanocomposites after the validation experiment was analyzed using one-way ANOVA and Duncan's multiple range test for statistical analysis.

Experiment Design and Optimization

Compression molding parameters were optimized by using face-centered central composite design (CCD) of response surface methodology (RSM). Varied parameters or variables are molding temperature (X_1), pressure (X_2), and duration (X_3) with a range of 150 to 200°C, 10 to 20 MPa, and 20 to 100 minutes, accordingly. The effect of variables on mechanical properties was investigated through determination of tensile strength (Y_1), yield strength (Y_2), elongation at break (Y_3), and Young's modulus (Y_4) as responses. The coded values

of three operating variables were set at three levels: -1 (minimum), 0 (central), and +1 (maximum) as shown in Table 1. A total of 20 experiments ($2^k + 2k + 6$) inclusive of 8 factorial points, 6 axial points and 6 center points were conducted where the alpha value was set to one.

Data were analyzed by using Design Expert statistical software (Version 7.0, Stat-Ease Inc. Minneapolis, MN, USA) where the significance of each variable and regression coefficients were evaluated by considering more than 95% confidence level ($P<0.05$) of variance analysis (ANOVA). The effect of variable on the responses was expressed in three dimensional (3D) and contour plot response surface in order to locate the optimal level. A second order polynomial equation was used to explain the system behavior as shown in Equation 1 where Y_1, Y_2, Y_3, and Y_4 are the responses and X_1, X_2, and X_3 are the variables influencing Y as response. The β_0 is the constant coefficient; β_1, β_2, β_3 are linear coefficients; β_{12}, β_{13}, β_{23} are interaction coefficients; and β_{11}, β_{22}, β_{33} are quadratic coefficients.

$$Y = \beta_0 + \beta_1X_1 + \beta_2X_2 + \beta_3X_3 + \beta_{12}X_1X_2 + \beta_{13}X_1X_3 + \beta_{23}X_2X_3 + \beta_{11}X_1^2 + \beta_{22}X_2^2 + \beta_{33}X_3^2 \quad \text{(Equation 1)}$$

Table 1
Central composite design matrix of coded and actual level of variables

Run	Temperature (°C), X_1		Pressure (MPa), X_2		Duration (min), X_3	
	Coded	Actual	Coded	Actual	Coded	Actual
1	0	175	0	15	0	60
2	+1	200	-1	10	+1	100
3	0	175	0	15	0	60
4	0	175	+1	20	0	60
5	0	175	0	15	-1	20
6	0	175	0	15	0	60
7	-1	150	-1	10	+1	100
8	0	175	0	15	0	60
9	-1	150	+1	20	+1	100
10	+1	200	+1	20	+1	100
11	+1	200	+1	20	-1	20
12	-1	150	0	15	0	60
13	+1	200	-1	10	-1	20
14	0	175	0	15	+1	100
15	0	175	0	15	0	60
16	+1	200	0	15	0	60
17	0	175	-1	10	0	60
18	-1	150	-1	10	-1	20
19	0	175	0	15	0	60
20	-1	150	+1	20	-1	20

Validation Experiment and Verification

The validity and adequacy of the regression models were proven by comparing the experimental data obtained and the fitted value predicted by the models.

RESULTS AND DISCUSSION

Preliminary Experiment and Range Selection

Selection of range was in accordance to the preliminary experiment of one-variable-at-time (OVAT) for molding duration, while temperature and pressure were selected based on literature. Temperature was ranged between 150°C to 200°C in consideration to melting temperature of UHMWPE which is approximately 140°C (Oral & Muratoglu, 2016) and the degradation temperature of CNF which is around 220°C (Yasim-Anuar et al., 2018). This is because cellulose degradation at high temperature could reduce the stiffness and strength of cellulose composite (Forsgren et al., 2020; Sapieha et al., 1989). Meanwhile, cellulose degradation was negligible at temperature below 200°C (Le Baillif & Oksman, 2009; Gan et al., 2020). Pressure range was set at 10 to 20 MPa as according to Wang & Ge (2007) and the range of duration was selected from 20 to 100 minutes based on the OVAT experiment conducted as shown in Figure 1. High tensile strength and elongation at break of UHMWPE/CNF bio-nanocomposites indicating less voids between UHMWPE granules and sufficient molding time were obtained after 20 minutes molding. Gradual reduction of elongation at break observed through further prolonged duration (60 to 100 minutes) proved appropriate selection of 60 minutes as a center point in between 20 to 100 minutes.

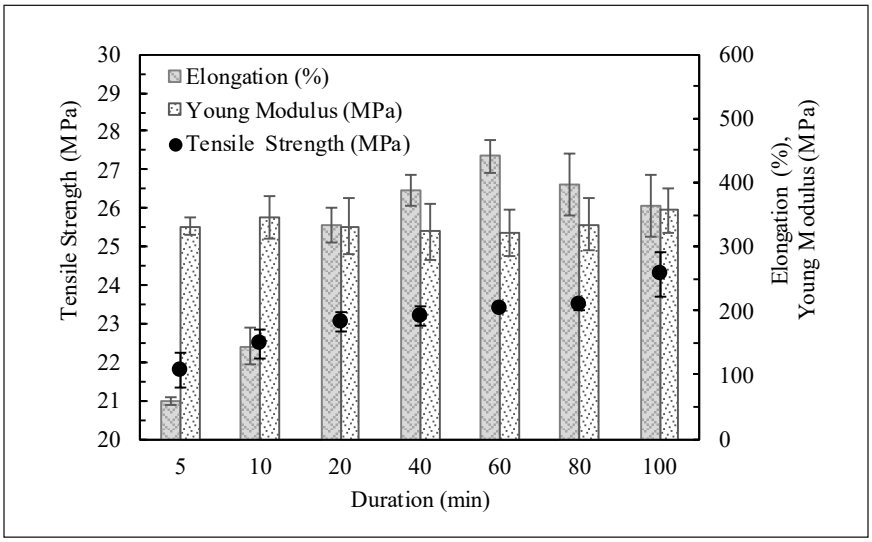

Figure 1. Mechanical properties of UHMWPE/CNF bio-nanocomposites as affected by duration at 175 °C and 15 MPa compression molding

Model Analysis

Table 2 shows the experimental and predicted values of the responses; tensile strength (Y_1), yield strength (Y_2), elongation at break (Y_3) and Young's modulus (Y_4). Natural log transformation was applied on elongation response as the best transformation suggested by the software. This was in consideration to the high maximum to minimum ratio of Y_3, values that were more than three (3.204).

The values obtained from Table 2 were subjected to analysis of variance (ANOVA) in order to select the model for each response, depending on the resulted significant model probability ($P<0.05$), insignificant lack-of-fit probability ($P>0.05$) and more than 80% coefficient of determination (R^2) (Bagheri et al., 2019; Warid et al., 2016). Full quadratic model was adopted as the best-fitted model where the results of ANOVA is tabulated in Table 3.

All models were found significant at the 5% confidence level where the *p*-values were all less than 0.05. The insignificant lack-of fit value ($P>0.05$) of all response models (0.9161,

Table 2
Experimental and predicted values of responses

Run	Tensile strength (MPa), Y_1		Yield strength (MPa)Y_2		Elongation (%), Y_3		Young's modulus (MPa), Y_4	
	*Exp	**Pred	*Exp	**Pred	*Exp	**Pred	*Exp	**Pred
1	25.4	24.8	22.6	22.7	480.3	457.6	0.346	0.343
2	22.8	22.9	23.1	23.1	243.8	238.7	0.361	0.356
3	25.1	24.8	22.7	22.7	473.1	457.6	0.341	0.343
4	24.3	24.3	22.5	22.7	393.9	397.4	0.334	0.337
5	25.0	24.8	22.7	22.7	425.3	436.7	0.347	0.344
6	23.5	24.8	22.9	22.7	455.7	457.6	0.341	0.343
7	25.9	25.9	21.4	21.3	299.0	294.6	0.325	0.333
8	25.0	24.8	22.7	22.7	496.8	457.6	0.333	0.343
9	27.1	27.4	21.3	21.3	371.9	366.8	0.322	0.320
10	22.8	22.5	23.1	23.1	155.1	155.8	0.378	0.378
11	23.6	23.7	23.3	23.2	216.2	215.5	0.366	0.359
12	27.3	26.9	21.4	21.6	385.8	404.7	0.353	0.341
13	23.7	23.5	23.5	23.5	274.4	273.3	0.359	0.362
14	24.8	24.9	22.2	22.4	380.5	398.0	0.339	0.338
15	24.3	24.8	23.3	22.7	468.3	457.6	0.349	0.343
16	23.7	24.0	23.2	23.3	265.9	272.2	0.361	0.369
17	23.5	23.4	22.9	22.9	376.7	401.0	0.351	0.344
18	24.1	24.4	22.0	21.9	262.4	256.5	0.364	0.364
19	25.0	24.8	22.7	22.7	440.0	457.6	0.340	0.343
20	26.6	26.5	21.6	21.6	384.6	385.9	0.321	0.327

*Exp: Experimental; **Pred: Predicted

Table 3
Analysis of variance (ANOVA) for response surface quadratic model

	Tensile strength (MPa), Y_1	Yield strength (MPa), Y_2	Ln Elongation (%), Ln Y_3	Young's Modulus (GPa), Y_4
Model - Quadratic	0.0006*	<0.0001*	<0.0001*	0.0026*
		Linear		
X_1 – Temperature	<0.0001*	<0.0001*	<0.0001*	0.0002*
X_2 – Pressure	0.0357*	0.2392	0.7711	0.1475
X_3 – Duration	0.7930	0.0195*	0.0122*	0.2387
		Interaction		
$X_1 X_2$	0.0407*	0.8171	<0.0001*	0.0102*
$X_1 X_3$	0.0255*	0.6101	0.0025*	0.0416*
$X_2 X_3$	0.4916	0.4619	0.0196*	0.0463*
		Quadratic		
X_1^2	0.0604	0.0548	<0.0001*	0.0339*
X_2^2	0.0212*	0.4529	0.0008*	0.6066
X_3^2	0.8692	0.2564	0.0094*	0.6430
Lack of Fit	0.9161**	0.7571**	0.3047**	0.1337**
R^2	0.9027	0.9463	0.9876	0.8642
Standard deviation	0.56	0.22	0.048	0.0078
Adequate precision	12.183	14.697	31.60	10.550

*statistically significant at $p < 0.05$ for model;
**statistically insignificant at $p > 0.05$ for lack of fit test

0.7571, 0.3047, and 0.1337, accordingly) indicated that each model could successfully predict and represent the data at points that was not included in the regression. This was also supported by high determination coefficients, R^2 by which the obtained values of 0.9027, 0.9463, 0.9876, and 0.8642 implied that 90%, 95%, 99% and 86% variance proportion of tensile strength, yield strength, elongation at break and Young's modulus are predictable by the model. As shown in Figure 2, predictions of all models were in a satisfactory match with the experimental value by which the proximity points were scattered along the fitted line. Additionally, the signal-to-noise ratio (adequate precision) of all response models were of greater than four, implying an adequate signal to navigate the design space including the estimation of the standard error of the predictions (Moradi et al., 2016).

Effect of the Compression Molding Variables on the Mechanical Properties of UHMWPE/CNF Bio-nanocomposites

The estimated regression coefficient explaining the variables effect on responses were expressed in equation follows, where Y_1, Y_2, Y_3, and Y_4 represent tensile strength, yield strength, elongation at break, and Young's modulus, respectively; and X_1, X_2, and X_3 are mixing temperature, pressure and duration, respectively.

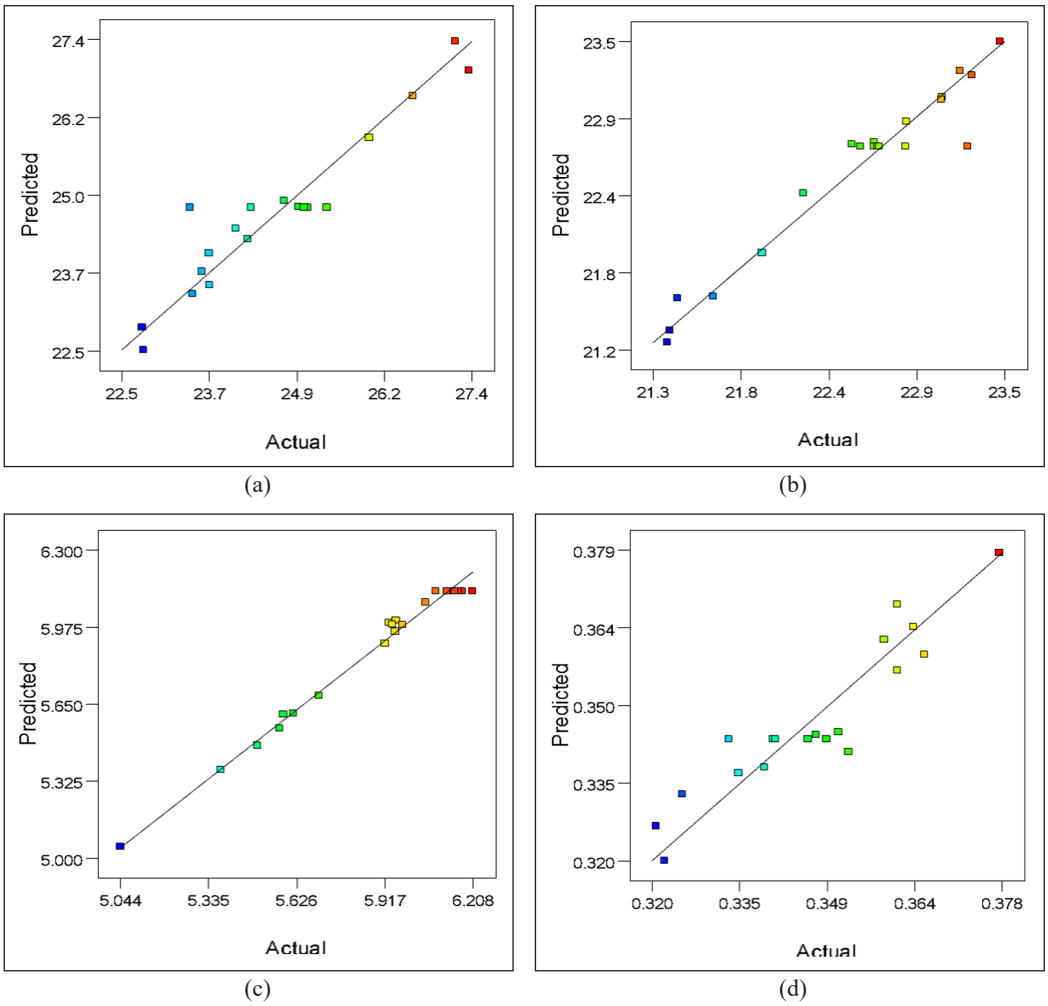

Figure 2. Experimental and predicted values for: (a) tensile strength; (b) yield strength; (c) elongation; and (d) Young's modulus of UHMWPE/CNF bio-nanocomposites

$$Y_1 = 24.76 - 1.44\ X_1 + 0.43\ X_2 + 0.048\ X_3 - 0.47\ X_1X_2 - 0.52\ X_1X_3 - 0.14\ X_2X_3 + 0.72\ X_1^2 - 0.93\ X_2^2 + 0.057\ X_3^2$$

(Equation 2)

$$Y_2 = 22.72 + 0.85\ X_1 - 0.085\ X_2 - 0.19\ X_3 + 0.018\ X_1X_2 + 0.04\ X_1X_3 + 0.058\ X_2X_3 - 0.28\ X_1^2 + 0.1\ X_2^2 - 0.16\ X_3^2$$

(Equation 3)

$$\text{Ln}\ (Y_3) = 6.13 - 0.2\ X_1 - 0.00456\ X_2 - 0.046\ X_3 - 0.16\ X_1X_2 - 0.068\ X_1X_3 - 0.047\ X_2X_3 - 0.32\ X_1^2 - 0.14\ X_2^2 - 0.093\ X_3^2$$

(Equation 4)

$$Y_4 = 0.34 + 0.014\ X_1 - 0.0039\ X_2 - 0.0031\ X_3 + 0.0087\ X_1X_2 + 0.0065\ X_1X_3 + 0.0063\ X_2X_3 + 0.012\ X_1^2 - 0.0025\ X_2^2 - 0.0023X_3^2$$

(Equation 5)

A perturbation plot was used to explain the individual effect of each variables on the responses studied. For instance, the coded units shown in Figure 3 represent the range of variables from -1.0 to +1.0 (*i.e.* 150°C to 200°C for temperature), whereby varied temperature and pressure gave significant linear effect on tensile strength. Increased temperature caused reduction of tensile strength whereby increased pressure up to 0.5 coded unit (17.5 MPa) led to increment of the response before reduced at higher pressure beyond 17.5 MPa.

The three-dimensional and contour plot of response surface showing interaction between variables against tensile strength according to Equation 2 is shown in Figure 4. Significant interaction effect of temperature and pressure was observed in which increased temperature along with pressure remarkably reduced the tensile strength (Figure 4a). In a similar manner, increased temperature along with increased duration of molding reduced the tensile strength despite insignificant linear effect of the later variable (Figure 4b). According to Xie et al. (2019), low temperature of compression molding may lead to insufficient impregnation of fillers and adjacent polymer chains while too high a temperature can lead to degradation. Meanwhile, longer duration could beneficially affected tensile strength due to improved resin flow and better fillers impregnation. Nevertheless, too long exposure to high temperature may also lead to degradation, hence explained the findings in this study by which highest tensile strength was obtained when UHMWPE/CNF bio-nanocomposites was molded at Run 9 (150°C, 15 MPa for 60 minutes) (Table 2). On the other hand, the lowest tensile strength was recorded in Run 2 (200°C, 10 MPa for 100 minutes).

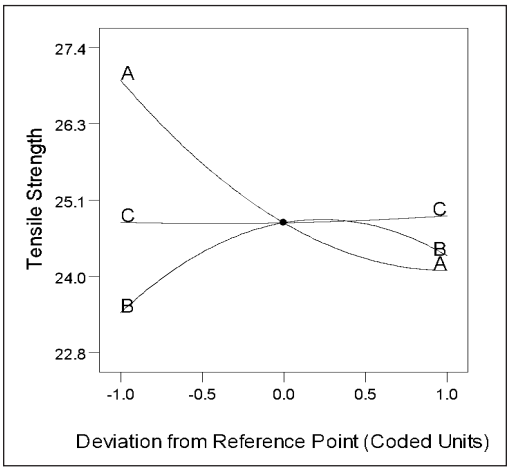

Figure 3. Perturbation plot of tensile strength in response to the changes of (A) temperature, (B) pressure, and (C) duration

In term of yield strength, no significant interaction between all variables was observed despite significant linear effect by temperature and duration (Table 3 and Figure 5a). Increased temperature from 150°C to 200°C (-1.0 to +1.0 coded unit) notably caused increment from approximately 21 MPa to 23 MPa. Prolonged duration from 20 to 60 minutes (-1.0 to 0 coded unit) gave no effect on yield strength but reduced when molded longer up to 100 minutes (+1 coded unit), possibly due to some thermal degradation attributed to long exposure to

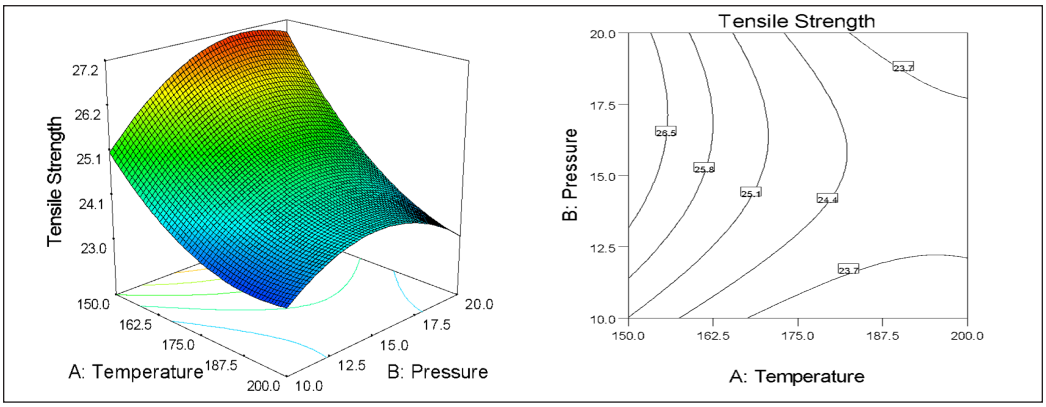

(a)

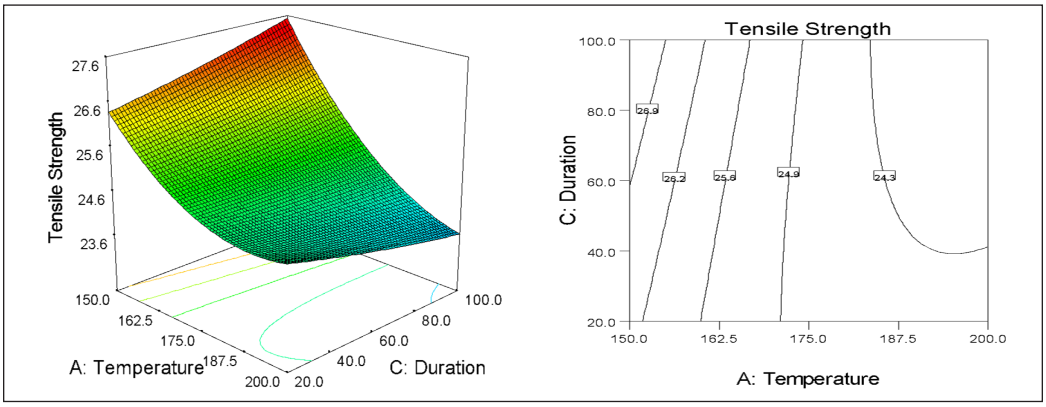

(b)

Figure 4. The 3D and contour plot for the dependence of UHMWPE/CNF bio-nanocomposite tensile strength on: (a) temperature and pressure; and (b) temperature and duration as significant variables

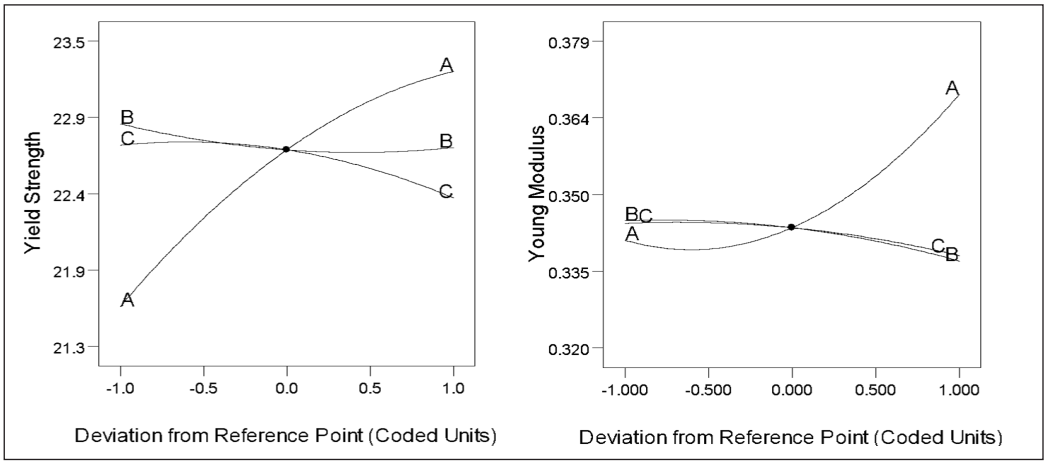

Figure 5. Perturbation plot of yield strength and Young's modulus in response to the changes of (A) temperature, (B) pressure and (C) duration

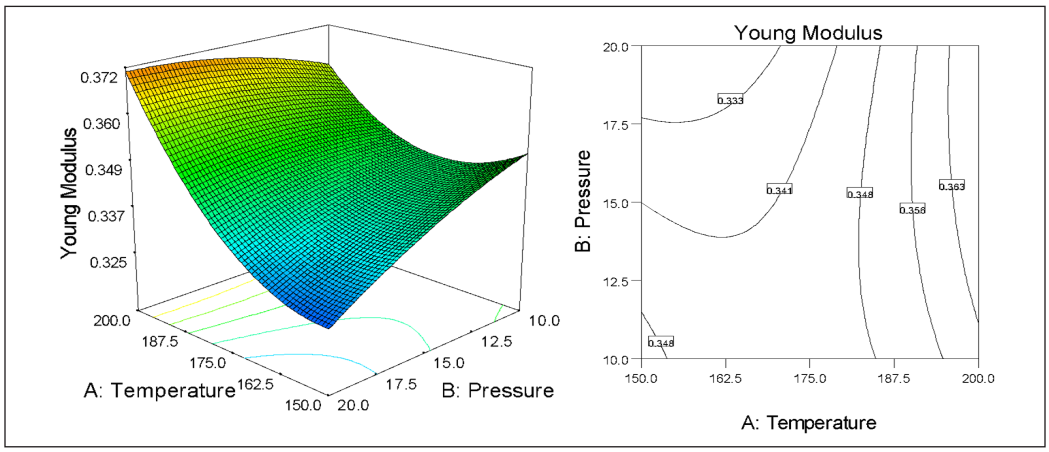

(a)

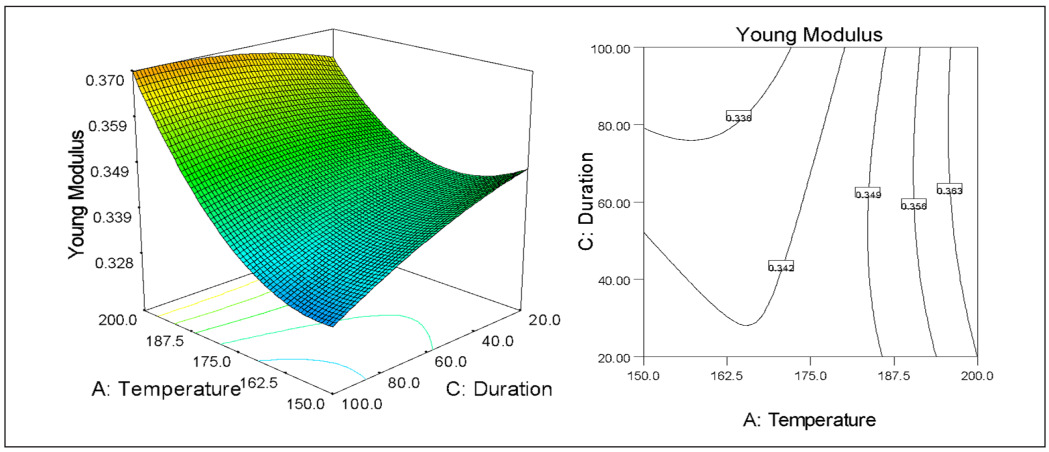

(b)

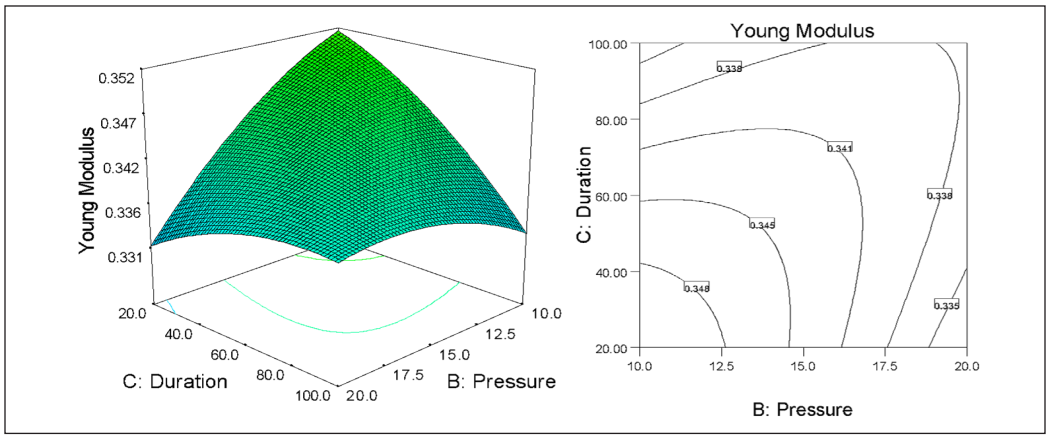

(c)

Figure 6. The 3D and contour plot for the dependence of UHMWPE/CNF bio-nanocomposite Young's modulus on: (a) temperature and pressure; (b) temperature and duration; and (c) pressure and duration as significant variables

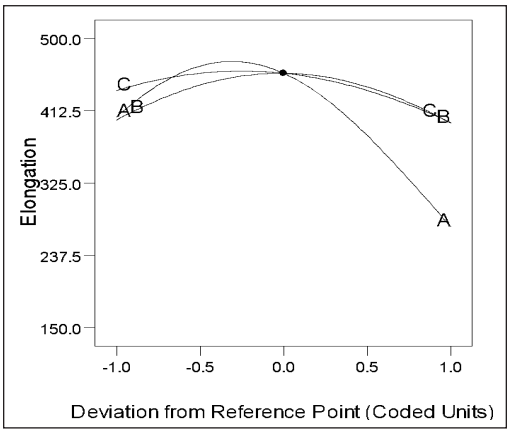

Figure 7. Perturbation plot of elongation at break in response to the changes of (A) temperature, (B) pressure and (C) duration

high temperature and pressure as previously described. In contrary, Young's modulus increased with increases of temperature (Figure 5b) while other variables gave no significant linear effect. Possible UHMWPE degradation was predicted due to exposure to high temperature and pressure. As degradation of polymer leads to formation of shorter chains that enable more packed crystals arrangement (Gleadall, 2015; Riley, 2012), higher crystallinity contributes to increases in Young's modulus (Doyle, 2000; Humbert et al., 2011). The synergistic effect of temperature with pressure, and temperature with duration on Young's modulus can also be seen in Figure 6a and Figure 6b, respectively, where Young's modulus increased along with increase values of the interacted variables. Inversely, the response value decreased by increases of pressure and duration as shown in Figure 6c.

The full quadratic model adopted comprised linear, interaction and quadratic terms indicating effect of variables on the respective response. For elongation at break, all model term listed were found to be significant except for linear pressure effect (Table 3). As shown in Figure 7, increased temperature and duration positively affected this response from -1.0 (lowest range) to -0.5 (162.5°C) and 0 (60 minutes) coded values, respectively. Further increase in both variables caused decrement in elongation at break, whereas interaction between all variables were significant as illustrated in three dimensional and contour plot of elongation break in Figure 8. The responses were in higher values when molded at temperature 162.5 to 175°C, 12.5 to 17.5 MPa and 40 to 60 minutes (Figure 8) suggesting that the optimal temperature for obtaining high elongation at break was within this range.

Response Surface Optimization of the Compression Molding Variables

Mechanical properties of UHMWPE/CNF bio-nanocomposites were notably affected by varied temperature, duration, interaction of other variables with temperature, duration, and pressure in descending order. The impact is however depended on the capability of polymer chains to undergo self diffusion that results in elimination of inter-particle voids beside avoidance of polymer degradation. An incomplete diffused UHMWPE particle/resin and CNF impregnation was expected to cause formation of voids or boundaries hence may act as cracks initiation site that afflicted the mechanical properties including tensile strength and elongation at break. As such, optimized temperature, duration and pressure play role in

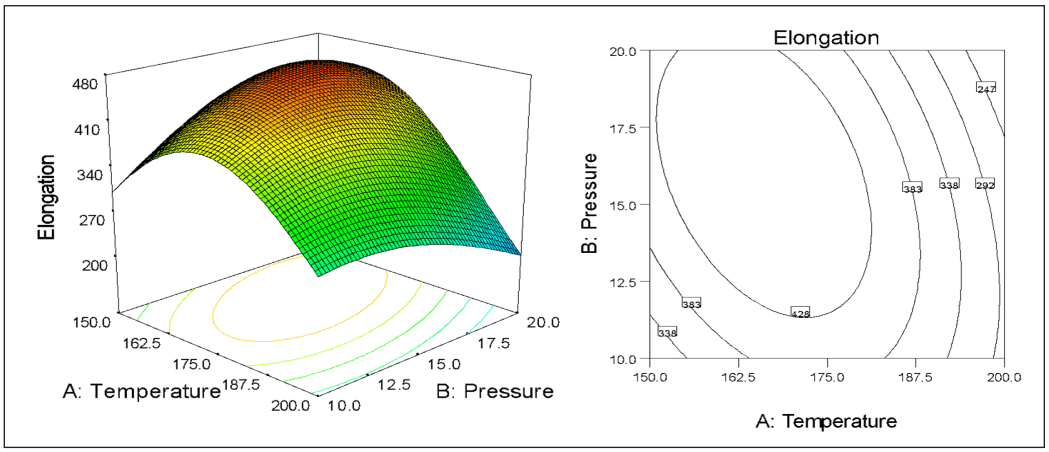

(a)

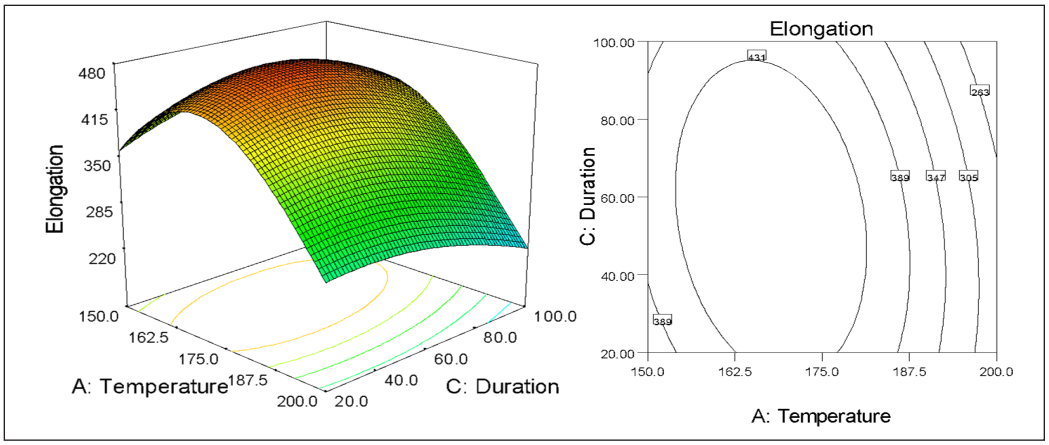

(b)

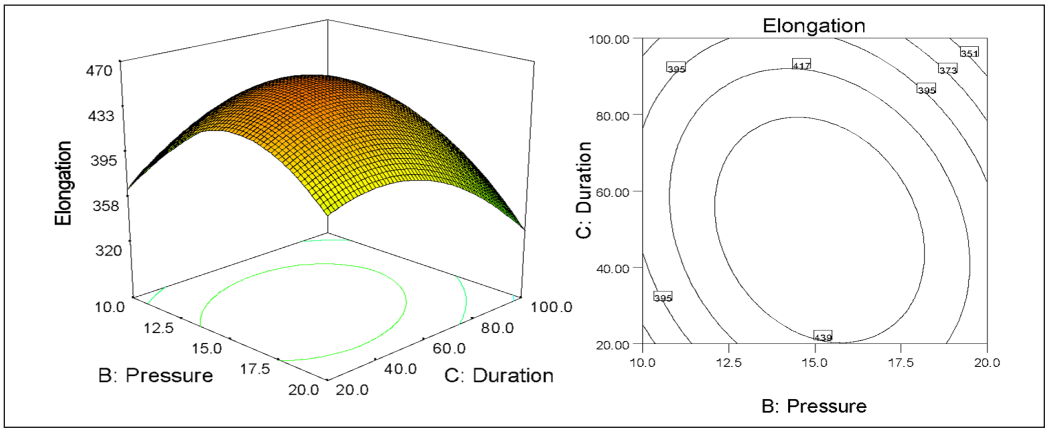

(c)

Figure 8. The 3D and contour plot for the dependence of UHMWPE/CNF bio-nanocomposite elongation at break on: (a) temperature and pressure; (b) temperature and duration; and (c) pressure and duration as significant variables

providing sufficient melt flow and time for UHMWPE polymer chains to allow complete consolidation and eliminates the boundaries through diffused adjacent chains. Additionally, adequate entanglement between adjacent chains could be established and translated into good mechanical properties.

A numerical optimization was conducted based on the design and the criteria of each variables as shown in Table 4. All mechanical properties were set to maximum except yield strength that was set in range. This was due to its small changes affected by varied temperature while other variables were insignificant. Optimum temperature, pressure and duration of compression molding were found to be at 180°C, 15 MPa and 20 minutes, respectively with desirability of 0.811. Verification experiment conducted proved the accuracy of the models where experimental value of all mechanical properties were in agreement with the predicted value by which all percent errors were less than 5% (Table 5).

Table 4
Numerical optimization criterion settings and solutions

Variables constraints								
Name		Goal		Lower limit		Upper limit		
X_1		is in range		150.0		200.0		
X_2		is in range		10.0		20.0		
X_3		minimize		20.0		100.0		
Response constraints								
Y_1		maximize		22.8		27.3		
Y_2		is in range		21.3		23.5		
Y_3		maximize		155.1		496.8		
Y_4		maximize		0.321		0.378		
Optimum Solutions								
No.	X_1	X_2	X_3	Y_1	Y_2	Y_3	Y_4	Desirability
1	180.0	15.0	20.0	24.6	22.9	420.1	0.346	0.811
2	180.5	15.0	20.0	24.6	22.9	417.9	0.346	0.809
3	180.0	17.5	20.0	24.6	22.9	408.1	0.341	0.787
3	180.0	10.0	20.0	23.2	23.1	362.7	0.352	0.681

Table 5
Comparison between predicted and experimental values of UHMWPE/CNF bio-nanocomposites fabricated at optimal conditions

	Predicted	Experimental	Percent error(%)
Tensile strength (MPa), Y_1	24.6	24.1 ± 1.1	1.92
Yield Strength (MPa), Y_2	22.9	23.3 ± 0.5	1.89
Elongation (%), Y_3	420.1	433.5 ± 26.2	3.22
Young Modulus (GPa), Y_4	0.346	0.361 ± 0.026	4.48

In addition, the optimized compression molding parameter obtained in this study was proven to provide comparable mechanical properties to the conventional process which required 45 minutes of molding duration. the duration of optimized condition was only 20 minutes which was less than two times shorter, hence could be favorable for industrial use (Table 6). Specifically, no significant different was observed on elongation and Young's modulus, while yield strength was only 2% higher. The tensile strength was however reduced from 28.0 MPa to 24.1 MPa.

Materials often experienced yielding, inelastic and plastic deformation before rupture. In order, the ability of materials to withstand load and undergo changes is determine through yield strength, Young's modulus and tensile strength. In light of UHMWPE utilization as load bearing materials such as joint arthroplasty component, yield strength is considered more important than tensile strength by which materials yielding under service condition is considered a failure (Fang et al., 2006). Moreover, the mechanical properties obtained from optimized molding conditions surpassed the minimal requirement of standard specification for consolidated UHMWPE for surgical implant (ASTM F648) which are 27 MPa, 19 MPa, and 250 % of tensile strength, yield strength and elongation, respectively (ASTM, 2014).

Table 6
Comparison between conventional and optimized compression molding

	Conventional (Kurtz et al., 1999)	**Optimized** (This study)
Temperature (°C)	175	180
Pressure (MPa)	15	15
Duration (min)	45	20
Tensile strength (MPa)	28.0 ± 1.851^{a}	24.1 ± 1.105^{b}
Yield strength (MPa)	22.8 ± 0.312^{b}	23.3 ± 0.536^{a}
Elongation (%)	461.6 ± 40.304^{a}	433.5 ± 26.242^{a}
Young's modulus (GPa)	0.366 ± 0.018^{a}	0.361 ± 0.026^{a}

CONCLUSIONS

In this paper, optimization of compression molding was conducted in order to reduce the long molding duration of UHMWPE. Optimum condition of molding UHMWPE/CNF bio-nanocomposites was 180°C, 15 MPa, and 20 minutes with more than 80% desirability, resulting in tensile strength, yield strength, elongation at break, and Young's modulus values of 22.83 MPa, 23.14 MPa, 487.31 %, and 0.391 GPa, accordingly. The mechanical properties of UHMWPE/CNF bio-nanocomposites obtained through optimized compression molding showed no significant different with pre-optimized molding whereas the molding time was successfully shortened by half through optimization. The findings suggest a more practical approach for UHMWPE bionanocomposites consolidation process.

ACKNOWLEDGEMENT

This study was funded by Ministry of Higher Education (MOHE, MALAYSIA) through HICoE research grant (Vot No.: 636911). The authors also gratefully acknowledge Universiti Putra Malaysia (UPM, MALAYSIA) and Japan Student Services Organization (JASSO, JAPAN) for provision of scholarship to the first author.

REFERENCES

ASTM. (2003). *Standard test method for tensile properties of plastics (D 638 - 02a)*. American Society for Testing and Materials. Penssylvania, USA. doi:10.1520/D0638-14.1

ASTM. (2014). ASTM F648: *Ultra-high-molecular-weight polyethylene powder and fabricated form for surgical implants, test, 1–9*. American Society for Testing and Materials. Penssylvania, USA. doi:10.1520/F0648-14

Bagheri, V., Ghanbarzadeh, B., Ayaseh, A., Ostadrahimi, A., Ehsani, A., Alizadeh-Sani, M., & Adun, P. A. (2019). The optimization of physico-mechanical properties of bionanocomposite films based on gluten/ carboxymethyl cellulose/ cellulose nanofiber using response surface methodology. *Polymer Testing*, *78*(July), 1-11. doi:10.1016/j.polymertesting.2019.105989

Campo, E. A. (2008). Mechanical properties of polymeric materials. In *Selection of polymeric materials,* (pp. 41–101). William Andrew: Norwich, USA. doi: 10.1016/B978-081551551-7.50004-8

Chukov, D. I., Stepashkin, A. A., Gorshenkov, M. V., Tcherdyntsev, V. V., & Kaloshkin, S. D. (2014). Surface modification of carbon fibers and its effect on the fiber-matrix interaction of UHMWPE based composites. *Journal of Alloys and Compounds*, *586*(SUPPL. 1), S459–S463. doi:10.1016/j.jallcom.2012.11.048

Doyle, M. J. (2000). On the effect of crystallinity on the elastic properties of semicrystalline polyethylene. *Polymer Engineering & Science*, *40*(2), 330–335. doi:10.1002/pen.11166

Fang, L., Leng, Y., & Gao, P. (2006). Processing and mechanical properties of HA/UHMWPE nanocomposites. *Biomaterials*, *27*(20), 3701–3707. doi:10.1016/j.biomaterials.2006.02.023

Forsgren, L., Berglund, J., Thunberg, J., Rigdahl, M., & Boldizar, A. (2020). Injection molding and appearance of cellulose-reinforced composites. *Polymer Engineering & Science*, *60*(1), 5–12. doi:10.1002/pen.25253

Fu, J., Ghali, B. W., Lozynsky, A. J., Oral, E., & Muratoglu, O. K. (2010). Ultra high molecular weight polyethylene with improved plasticity and toughness by high temperature melting. *Polymer*, *51*(12), 2721–2731. doi:10.1016/j.polymer.2010.04.003

Gan, P. G., Sam, S. T., Abdullah, M. F. bin, & Omar, M. F. (2020). Thermal properties of nanocellulose-reinforced composites: A review. *Journal of Applied Polymer Science*, *137*(11), 1-14. doi:10.1002/app.48544

Gao, G., & Fu, J. (2019). Highly crosslinked UHMWPE for joint implants. In Fu, J., Jin, Z.-M., & Wang, J. W. (Ed.), *UHMWPE biomaterials for joint implants: Structures, properties and clinical performance* (pp. 21–68). Singapore: Springer. doi: 10.1007/978-981-13-6924-7_2

Gleadall, A. (2015). Mechanical properties of biodegradable polymers for medical applications. In Pan, J. (Ed.), *Modelling degradation of bioresorbable polymeric medical devices* (pp. 163–199). Manchester, United Kingdom: Woodhead Publishing. doi: 10.1533/9781782420255.2.163

Humbert, S., Lame, O., Séguéla, R., & Vigier, G. (2011). A re-examination of the elastic modulus dependence on crystallinity in semi-crystalline polymers. *Polymer*, *52*(21), 4899–4909. doi:10.1016/j.polymer.2011.07.060

Khalil, Y., Kowalski, A., & Hopkinson, N. (2016). Influence of energy density on flexural properties of laser-sintered UHMWPE. *Additive Manufacturing*, *10*, 67–75. doi:10.1016/j.addma.2016.03.002

Kurtz, S. M. (2016a). A primer on UHMWPE. In *UHMWPE biomaterials handbook: Ultra high molecular weight polyethylene in total joint replacement and medical devices: Third edition* (pp. 1–6). Waltham, USA: William Andrew. doi: 10.1016/B978-0-12-374721-1.00001-8

Kurtz, S. M. (2016b). From ethylene gas to UHMWPE component: The process of producing orthopedic implants. In *UHMWPE biomaterials handbook: Ultra high molecular weight polyethylene in total joint replacement and medical devices: Third edition* (pp. 7-20). Waltham, USA: William Andrew. doi: 10.1016/B978-0-323-35401-1.00002-8

Kurtz, S. M., Muratoglu, O. K., Evans, M., & Edidin, A. A. (1999). Advances in the processing, sterilization, and crosslinking of ultra-high molecular weight polyethylene for total joint arthroplasty. *Biomaterials*, *20*(18), 1659–1688. doi: 10.1016/s0142-9612(99)00053-8

Le Baillif, M., & Oksman, K. (2009). The effect of processing on fiber dispersion, fiber length, and thermal degradation of bleached sulfite cellulose fiber polypropylene composites. *Journal of Temoplastic Composite Materils*, *22(2)*, 115–133. doi:10.1177/0892705708091608

Li, Y., He, H., Huang, B., Zhou, L., Yu, P., & Lv, Z. (2017). In situ fabrication of cellulose nanocrystal-silica hybrids and its application in UHMWPE: Rheological, thermal, and wear resistance properties. *Polymer Composites, 39*(S3), 1–13. doi:10.1002/pc.24690

Moradi, M., Fazlzadehdavil, M., Pirsaheb, M., Mansouri, Y., Khosravi, T., & Sharafi, K. (2016). Response surface methodology (RSM) and its application for optimization of ammonium ions removal from aqueous solutions by pumice as a natural and low cost adsorbent. *Archives of Environmental Protection*, *42*(2), 33–43. doi:10.1515/aep-2016-0018

Oral, E., & Muratoglu, O. K. (2016). Highly cross-linked UHMWPE doped with vitamin E. In Kurtz, S. M. (Ed.) *UHMWPE Biomaterials handbook: Ultra high molecular weight polyethylene in total joint replacement and medical devices: Third edition* (pp. 307–325). Waltham, USA: William Andrew. doi: 10.1016/B978-0-323-35401-1.00018-1

Parasnis, N. C., & Ramani, K. (1998). Analysis of the effect of pressure on compression moulding of UHMWPE. *Journal of Materials Science: Materials in Medicine*, *9*(3), 165–172. doi:10.1023/A:1008871720389

Paxton, N. C., Allenby, M. C., Lewis, P. M., & Woodruff, M. A. (2019). Biomedical applications of polyethylene. *European Polymer Journal*, *118*, 412-428. doi: 10.1016/j.eurpolymj.2019.05.037

Raghuvanshi, S. K., Ahmad, B., Siddhartha, Srivastava, A. K., Krishna, J. B. M., & Wahab, M. A. (2012). Effect of gamma irradiation on the optical properties of UHMWPE (Ultra-high-molecular-weight-polyethylene) polymer. *Nuclear Instruments and Methods in Physics Research, Section B: Beam Interactions with Materials and Atoms*, *271*, 44–47. doi:10.1016/j.nimb.2011.11.001

Riley, A. (2012). Basics of polymer chemistry for packaging materials. In Emblem, A. & Emblem, H. (Ed.), *Packaging technology* (pp. 262–286). Cambridge, England: Woodhead Publishing. doi: 10.1533/9780857095701.2.262

Sapieha, S., Pupo, J. F., & Schreiber, H. P. (1989). Thermal degradation of cellulose-containing composites during processing. *Journal of Applied Polymer Science*, *37*(1), 233–240. doi:10.1002/app.1989.070370118

Wang, J., Cao, C., Yu, D., & Chen, X. (2018). Deformation and stress response of carbon nanotubes/ UHMWPE composites under extensional-shear coupling flow. *Applied Composite Materials*, *25*(1), 35–43. doi:10.1007/s10443-017-9606-8

Wang, S., & Ge, S. (2007). The mechanical property and tribological behavior of UHMWPE: Effect of molding pressure. *Wear*, *263*(7–12), 949–956. doi:10.1016/j.wear.2006.12.070

Wang, S., Feng, Q., Sun, J., Gao, F., Fan, W., Zhang, Z., ... & Jiang, X. (2016). Nanocrystalline cellulose improves the biocompatibility and reduces the wear debris of ultrahigh molecular weight polyethylene via weak binding. *ACS Nano*, *10*(1), 298–306. doi:10.1021/acsnano.5b04393

Warid, M. N. M., Ariffin, H., Hassan, M. A., & Shirai, Y. (2016). Optimization of superheated steam treatment to improve surface modification of oil palm biomass fiber. *BioResources, 11*(3), 5780-5796. doi:10.15376/ biores.11.3.5780-5796

Xie, J., Wang, S., Cui, Z., & Wu, J. (2019). Process optimization for compression molding of carbon fiber–reinforced thermosetting polymer. *Materials*, *12*(15), 2-13. doi:10.3390/ma12152430

Yasim-Anuar, T. A. T., Ariffin, H., & Hassan, M. A. (2018). Characterization of cellulose nanofiber from oil palm mesocarp fiber produced by ultrasonication. *IOP Conference Series: Materials Science and Engineering*, *368*(1), 1-11. doi:10.1088/1757-899x/368/1/012033